# Second harmonic generation in reflection from crystalline GaAs under intense picosecond laser irradiation

A. M. Malvezzi, J. M. Liu, and N. Bloembergen

Citation: Appl. Phys. Lett. **45**, 1019 (1984); doi: 10.1063/1.95047
View online: https://doi.org/10.1063/1.95047
View Table of Contents: http://aip.scitation.org/toc/apl/45/10
Published by the American Institute of Physics

**Articles you may be interested in**

ENHANCEMENT OF OPTICAL SECOND-HARMONIC GENERATION (SHG) BY REFLECTION PHASE MATCHING IN ZnS AND GaAs
Applied Physics Letters **8**, 313 (1966); 10.1063/1.1754454

COMSOL CONFERENCE
2018 BOSTON
Discover the power of multiphysics simulation.

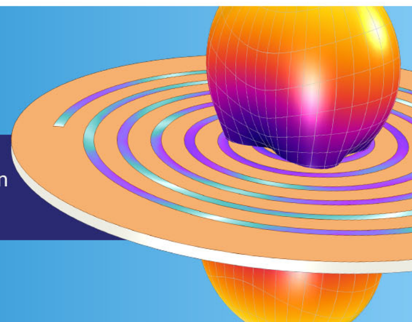

# Second harmonic generation in reflection from crystalline GaAs under intense picosecond laser irradiation

A. M. Malvezzi
*Division of Applied Sciences, Harvard University, Cambridge, Massachusetts 02138*
J. M. Liu
*GTE Laboratories, Incorporated, Waltham, Massachusetts 02254*
N. Bloembergen
*Division of Applied Sciences, Harvard University, Cambridge, Massachusetts 02138*

(Received 18 June 1984; accepted for publication 27 August 1984)

The emission of second harmonic radiation in reflection from crystalline GaAs irradiated with 20-ps, 530-nm laser pulses has been measured for incident laser fluences far exceeding the threshold fluence $F_{th}$ for permanent reflectivity changes. The results are consistent with the occurrence of surface melting during the laser pulse. Detailed analysis of the second harmonic signals reveals an upper limit of 2 ps for the structural transition associated with the melting of the surface.

The intensity of second harmonic generation (SHG) from noncentrosymmetric crystals such as GaAs should show a drastic decrease when a transition to a centrosymmetric phase occurs. This has been observed with nanosecond resolution by Akhmanov *et al.*[1] when the laser fluence exceeds a threshold value for melting.

In this letter we present the results of SHG study on GaAs with picosecond excitation. In simple single shot experiments, the SHG dependence of the incident laser fluence is monitored under appropriate geometrical conditions. The deviation from the quadratic power law is analyzed by model calculations based on the assumption of a transition to a centrosymmetric phase as soon as a critical fluence during the 20-ps laser pulse is accumulated on the surface of GaAs.

In our analysis we use mainly (110) surfaces excited with single picosecond pulses at 532 nm with the direction of the electric field parallel to a ⟨111⟩ crystal direction. The second harmonic from a passively mode-locked Nd:yttrium aluminum garnet laser system is focused on the GaAs surface at an angle of 45° of incidence. The pulse duration is $t = 12.5$ ps at the $1/e$ points of the Gaussian temporal profile. The second harmonic signal at 266 nm is detected in the direction of specular reflection by a photomultiplier tube. The reflected exciting radiation is suppressed by a combination of filters. Second harmonic signals down to $\simeq 200$ photons are detected. The inherent fluctuations in the pulse duration of the laser pulse are monitored by standard $\tau A$ techniques.[2] Accidental double pulses are rejected. Both precautions yield a significant smoothing of the SHG data.

Generally, two separate SHG regimes are observed. Below the critical fluence of 30 mJ/cm$^2$ at 532 nm, where melting and subsequent amorphization of the surface occur, the signal exhibits the expected quadratic power law dependence $I_s = \eta_o I_g^{\,2}$, where $I_s$ is the intensity of the second harmonic pulse and $I_g$ is the intensity of the exciting green pulse. Figure 1 shows a log-log plot of the absolute SHG energy emitted from a (110) surface as a function of the excitation fluence $F$. The data in this figure are integrated signals over space and time. The excitation pulse is focused to a spot size of 200 $\mu$m in diameter. The SHG energy increases with slope 2 up to fluence level of $F_{th} = 30$ mJ/cm$^2$. The SHG efficiency is not sensibly affected by the generation of a dense electron-hole plasma or by lattice heating up to the melting point. A value of $\eta_0 = 2.5 \times 10^{-18}$ cm$^2$/W is derived from the experiment. Above $F_{th}$ the SHG signal grows more slowly. The noncentrosymmetric GaAs structure is obviously changed during the excitation pulse. The threshold fluence value of 30 mJ/cm$^2$ is in excellent agreement with calculated fluence levels necessary to melt GaAs surfaces.[3] The solid curve in Fig. 1 represents calculated SHG values where a cutoff in the SHG efficiency is assumed as soon as the critical fluence $F_{th}$ is accumulated during the pulse. The integration

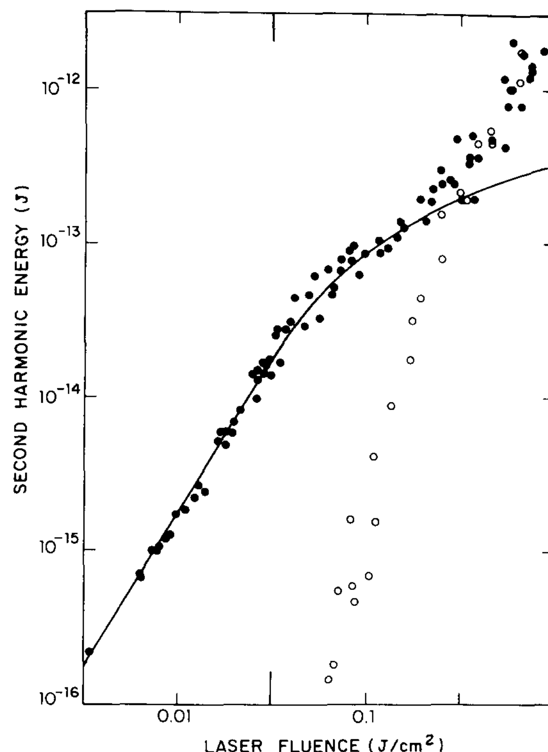


FIG. 1. Energy of the specular emission at 266 nm vs incident laser fluence ($\lambda = 532$ nm) on GaAs. The laser spot diameter is 200 $\mu$m. Closed dots refer to (1$\bar{1}$0) surface, laser electric field parallel to the [1$\bar{1}$1] crystal axis. Open dots refer to (100) crystal surface, laser electric field parallel to the [001] crystal axis. The solid curve represents calculated SHG energy with $\tau_s = 0$ as discussed in the text.

 © 1984 American Institute of Physics 

over the Gaussian space and time profiles smooths the sharp drop of SHG emission considerably. At fluences far above the threshold value, $F_{th}$, for melting the UV signal increases again. This puzzling behavior has been carefully examined by looking at the angular and time dependence of the signal. For pump fluences exceeding $\simeq 3F_{th}$ an additional UV signal is detected, whose fully isotropic angular distribution is in marked constrast to the specular SHG beam. This radiation, which is accompanied at high fluences by a readily observed blue spark at the surface, exhibits a decay time of $\simeq 1\ \mu$s, while the duration of the SHG signal is limited by the time constant (10 ns) of the photomultiplier tube. To analyze the growth of this additional signal, the emission from a (100) GaAs surface is studied, where the polarization of the excitation beam is kept parallel to a $\langle 001 \rangle$ axis. Under these conditions, the SHG signal is zero and the background UV emission can be measured as a function of the exciting 532-nm pulse fluence. As shown in Fig. 1, this new emission does not affect the SHG signal at fluences below $5F_{th}$. However, due to the extreme nonlinear behavior, it is responsible for the unexpected increase of the UV emission at higher fluences. A further study of this new emission process, which is closely related to the evaporation and plasma formation in front of the surface, is beyond the scope of this letter. Here, we restrict our interest to the time scale on which the surface structural changes on GaAs occur. For this purpose, this isotropic contribution at high pump fluences is simply subtracted from the total UV signal on (110) surfaces.

To enhance the deviation from the quadratic power law above $F_{th}$ the spatial resolution of the experimental setup is improved by inserting a diaphragm in the path of the specular SHG beam. In Fig. 2, the energy dependence of the SHG emitted by the central portion (120 $\mu$m in diameter) of the excited area on the surface is shown. Clearly, the saturation of the time integrated SHG signal in the vicinity of $F_{th}$ is more pronounced. These data are now compared with model calculations, where the transition from an ordered noncentrosymmetric structure to a disordered liquid phase is simulated by a SHG efficiency decaying with a time constant $\tau_s$. The SHG intensity is given by

$$I_s(r,t) = \eta(r,t) I_g^2(r,t),$$

where

$$\eta(r,t) = \begin{cases} \eta_0 & \text{for } t < t_m(r) \\ \eta_0 \exp\left( - \dfrac{t - t_m(r)}{\tau_s} \right) & \text{for } t > t_m(r). \end{cases}$$

At each point $r$ on the surface, $\eta$ starts to decay as soon as the critical fluence $F_{th}$ is reached

$$\int_{-\infty}^{t_m(r)} I_g(r,t)\, dt = F_{th}.$$

The solid curve in Fig. 2 corresponds to a stepwise truncation of the SHG emission by setting $\tau_s = 0$. Around the threshold value for melting, when the phase transition still occurs on the trailing edge of the excitation pulse, the data are well described by the curve. However, at higher fluences, when $F_{th}$ is reached during the leading part of the excitation pulse, the SHG data points are slightly above the calculated curve.

In order to further elucidate the temporal behavior of the transition to the disordered phase the data of Fig. 2 are represented in a linear scale in Fig. 3 and compared with the model calculations with different time constants $\tau_s$. Despite

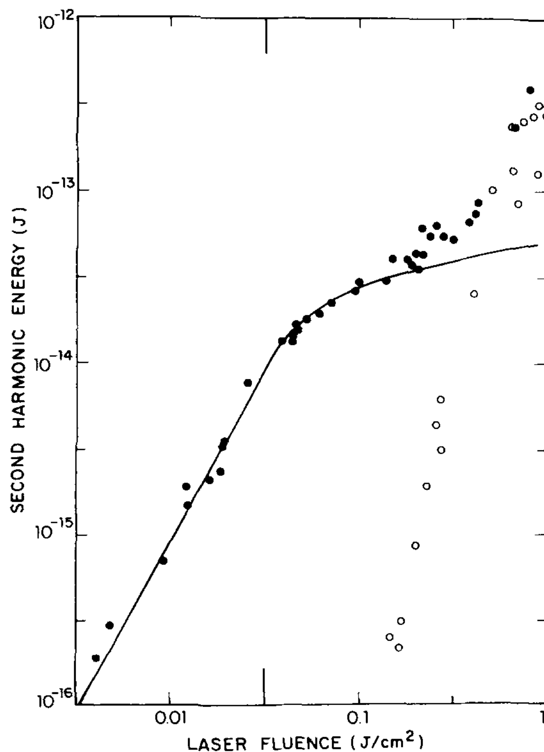


FIG. 2. Same as Fig. 1, but limiting the collection of the SHG signal from a disk of 120 $\mu$m in diameter centered on the incident laser spot.

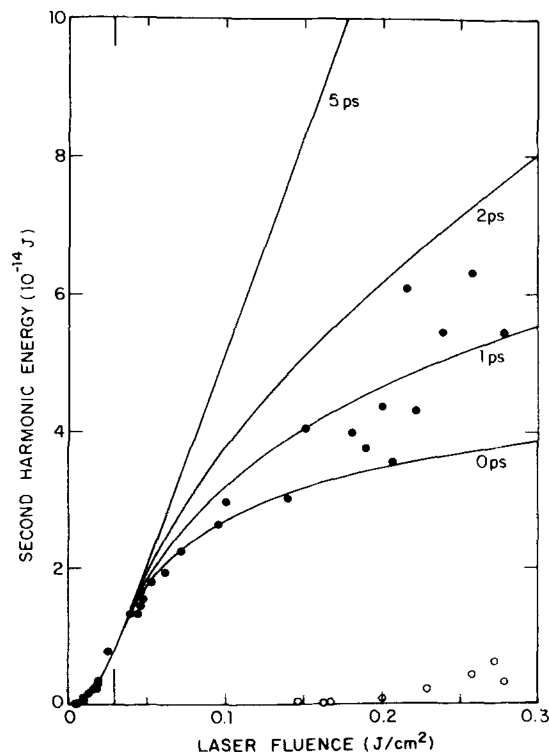


FIG. 3. Plot of the data of Fig. 2 on linear scales. The solid curves refer to calculations with the values of $t_s$ shown.

the scattering of the data points the solid curves of Fig. 3 show clearly that the SHG emission drops with a time constant $\tau_s < 2$ps as soon as the energy necessary for melting is locally delivered. In Fig. 3, the calculation for $\tau_s = 5$ ps is also shown, demonstrating the sensitivity of the SHG emission process towards a slightly delayed phase transition.

In conclusion, the SHG results obtained with a single beam technique indicate that an ultrafast transition to a centrosymmetric phase occurs in crystalline GaAs under picosecond laser irradiation. The SHG emission follows the usual quadratic power law up to the threshold fluence for melting. Above this level the data are consistent with an ultrafast transition to a disordered phase within 2 ps.

We would like to thank R. Yen and J. Y. Tsao for providing the (110) GaAs samples, H. Kurz and D. von der Linde for illuminating discussions. This research was supported by the Office of Naval Research under contract No. 0014-83K-0030 and the Joint Service Electronic Program under contract No. N00014-75-C-0648.

[1]S. A. Akhmanov, N. I. Koroteev, G. A. Paition, I. L. Shumay, M. F. Guljautdinov, I. B. Khaibullin, and E. I. Shtyrkov, Op. Commun, **47**, 202 (1983).
[2]W. L. Smith and J. H. Bechtel, J. Appl. Phys. **47**, 1065 (1976).
[3]A. Lietoila and J. F. Gibbons, in *Laser and Electron-Beam Interactions with Solids*, edited by B. R. Appleton and G. K. Celler (North-Holland, New York, 1982), p. 163.

# A new, highly multiplexable liquid crystal display

T. J. Scheffer and J. Nehring
*Brown Boveri Research Center, CH-5405 Baden, Switzerland*

(Received 11 July 1984; accepted for publication 29 August 1984)

A new, highly multiplexable liquid crystal display is described, which has a superior image quality than a twisted nematic display multiplexed at the same high level. The display cell consists of a chiral-doped nematic layer with tilted boundaries and a twist angle of $\sim 270°$. It operates in a birefringent optical mode between two "nonconventionally" oriented polarizers. Performance characteristics presented for a $120 \times 240$ dot matrix panel multiplexed at a 1/120 duty cycle include driving voltages compatible with complementary-metal-oxide-semiconductor technology, 300-ms response times, a contrast ratio of 10:1 at normal incidence, and $\geqslant$4:1 inside a viewing cone of 45° from the vertical.

Recent market studies predict an enormous growth in the demand for liquid crystal displays (LCD's) with large information capacities, particularly for use with portable computers. Present LCD's used in portable computers are of the twisted nematic (TN) variety[1] which have been optimized for high information content. However, the contrast ratio of these displays is limited and the viewing angle is narrow.

The aforementioned limitations of the TN effect used in high information content LCD's have motivated the investigation and development of alternative LCD technologies and electro-optical effects. The purpose of this letter is to report briefly the principle and performance of a LCD that uses a new electro-optical effect which has a much better image quality than a TN display multiplexed at the same high level. In this letter we refer to this new effect as the "supertwisted birefringence effect" (SBE) because the layer twist angle is about three times larger than in a TN display and the contrast results from the interference of the two optical normal modes rather than from the guiding of a single mode. Figure 1 shows a schematic view of a reflective SBE display. The fundamental differences in cell construction between the SBE display and a conventional TN display are a $\sim 270°$ liquid crystal twist angle, high-pretilt orientation layers, and nonconventional orientation of the polarizers. In contrast to the 270° device reported by Waters *et al.*,[2] the SBE display contains no pleochroic dyes and uses two polarizers.

It is known that the bistable range of a twisted nematic

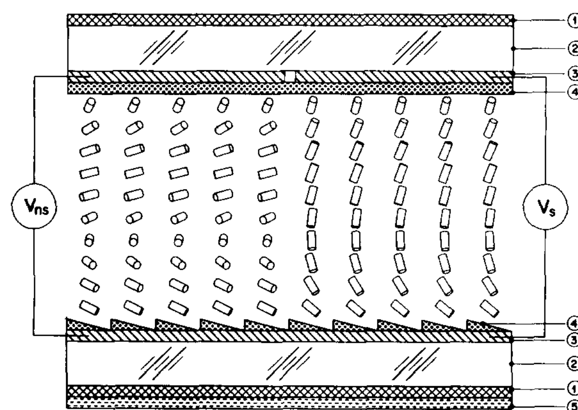


FIG. 1. Schematic view of a reflective SBE matrix display with a left-handed twist angle of 270° showing the orientation of the local optic axis with applied select and non-select rms voltages $V_s$ and $V_{ns}$. 1 = polarizer, 2 = glass plate, 3 = transparent electrode, 4 = high-pretilt orientation layer, 5 = reflector.

 © 1984 American Institute of Physics 